Association of Branched Nucleic Acids: Structural and Physicochemical Analysis of Antiparallel T·AT Triple-Helical DNA⊥

Robert H. E. Hudson,†,‡ André H. Uddin,‡,§ and Masad J. Damha*,§

Contribution from the Departments of Chemistry, McGill University, Montreal, Quebec H3A 2K6, Canada, and Erindale College, University of Toronto, Mississauga, Ontario L5L 1C6, Canada

Received August 7, 1995®

Abstract: We report the first example of a stable triple-stranded helix consisting of *exclusively* T·AT (reverse-Hoogsteen·Watson−Crick) base triplets. The orientation of the third (T) strand in this triplex is *anti-parallel* with respect to the purine strand of the underlying duplex. Previous studies have examined the formation of these "antiparallel" T·AT triplets within a G·GC-rich environment; however, the present study demonstrates that G·GC triplets are not a requirement. Our approach to induce and stabilize the antiparallel triplex involves the use of a branched oligonucleotide with two parallel dT_{10} strands joined to riboadenosine via 2′−5′ and 3′−5′ phosphodiester linkages, *i.e.*, $rA^{[2'-5'\text{-}dT10]}3'-5'\text{-}dT_{10}$ (**1**) (Hudson, R. H. E.; Damha, M. J. *J. Am. Chem. Soc.* **1993**, *115*, 2119−2124). This triplex was further stabilized by $MgCl_2$ or NaCl at neutral pH. Triple helix formation by branched oligonucleotide **1** and dA_{10} was investigated by thermal denaturation analysis and circular dichroism spectroscopy. The melting curves at 260 and 284 nm show a single transition from bound to unbound species, indicative of cooperative melting. A linear oligonucleotide with a loop made of four dC residues between two dT_{10} strands, and with a 5′−5′-phosphodiester linkage at one of the C/T_{10} junctions, i.e., $3'\text{-}dT_{10}C_4\text{-}5'-5'\text{-}dT_{10}\text{-}3'$, did not form a similar triple helical structure. This result shows that the conformational rigidity imparted to the pyrimidine strands, by the branch point in **1**, serves to preorganize and stabilize the complex. Potassium ions inhibited triplex helix formation. In accord with what has been demonstrated previously for "parallel" Py·PuPy (Hoogsteen−Watson−Crick) triplexes, we show that short oligoadenylates (i.e., dA_4 and dA_5) can bind *cooperatively* to the branched oligomer **1**. The triplex-inducing capacity of branched oligonucleotides has potentially important implications in the study of intramolecular triplexes that occur *in vivo*.

Introduction

Triple-stranded helical nucleic acids were first recognized nearly 40 years ago, shortly after the elucidation of the structure of double-stranded DNA.[1] Even so, triplexes remained a structural curiosity until recently, when it was shown that small synthetic oligonucleotides were able to bind to duplex DNA in a sequence-specific manner.[2] The discovery of triplex-containing structures that may exist *in vivo* and may play a role in mediating cellular events has further stimulated interest in triple-helical DNA.[3] With the advent of NMR spectroscopic techniques as well as in-depth thermodynamic and molecular dynamic studies, a much better understanding of the structure and properties of these molecules is being realized.[4] Undoubtedly, a major factor contributing to these developments is the facility with which synthetic oligonucleotides and their analogs are available today.[5] Oligonucleotide-directed triple helix formation offers the possibility of developing therapeutic agents capable of site-specific inhibition of transcription *in vivo* and remains an active area of research ("antigene" strategy).[6] Another area that has received significant experimental attention is the sequence-specific recognition of single-stranded DNA[7] and RNA[8] by triple-helix formation. This more recent and

* To whom correspondence should be addressed: Otto Maass Chemistry Building, Department of Chemistry, McGill University, 801 Sherbrooke St. West, Montreal, QC H3A 2K6, Canada. E-mail: damha@omc.lan.mcgill.ca. Tel. (514) 398-7552. Fax: (514) 398-3797.

⊥ Dedicated to Professor Robert L. Letsinger on the occasion of his 75th birthday.

† University of Toronto. Current address: Beckman Institute, California Institute of Technology, Pasadena, CA 91125.

§ McGill University.

‡ Both R.H.E.H. and A.H.U. contributed equally to this work, which was performed in partial fulfillment of the requirements for a Ph.D. degree, Faculty of Graduate Studies and Research, McGill University, Montreal, and University of Toronto, Toronto, Canada.

® Abstract published in *Advance ACS Abstracts*, December 1, 1995.

(1) (a) Felsenfeld, G.; Davies, D. R.; Rich, A. J. *J. Am. Chem. Soc.* **1957**, *79*, 2023−2024. (b) Riley, M.; Mailing, B.; Chamberlin, M. J. *J. Mol. Biol.* **1966**, *20*, 359−389. (c) Michelson, A. M.; Massoulie, J.; Gushchelbauer, W. *Prog. Nucl. Acid Res. Mol. Biol.* **1967**, *6*, 83−141. (d) Morgan, A. R.; Wells, R. D. *J. Mol. Biol.* **1968**, *37*, 63−80.

(2) (a) Moser, H. E.; Dervan, P. B. *Science* **1987**, *238*, 645−650. (b) Le Doan, T.; Perrouault.; Praseuth, D.; Habhoub, N.; Decout, J. L.; Thoung, N. T.; Lhomme, J.; Hélène, C. *Nucleic Acids Res.* **1987**, *15*, 7749−7760.

(3) (a) Mirkin, S. M.; Lyamichev, V. I.; Drushlyak, K. N.; Dobrynin, V. N.; Filipov, S. A.; Frank-Kamenetskii, M. D. *Nature* **1987**, *330*, 495−497. (b) For a review, see: Wells, R. D.; Collier, D. A.; Hanvey, J. C. Shimizu, M.; Wohlrab, F. *FASEB J.* **1988**, *2*, 2939−2949.

(4) (a) Plum, G. E.; Pilch, D. S.; Singleton, S. F.; Breslauer, K. J. *Annu. Rev. Biophys. Biomol. Struct.* **1995**, *24*, 319−350 and references therein. (b) Sekharudu, C. Y.; Yathindra, N.; Sundaralingam, M. In *Structural Biology: The State of the Art*; Sarma, R. H., Sarma, M. H., Eds.; Adenine Press: Guilderland, NY, 1994; pp 113−125.

(5) (a) Letsinger, R. L.; Lunsford, W. B. *J. Am. Chem. Soc.* **1976**, *98*, 3655−3661. (b) Beaucage, S.; Caruthers, M. H. *Tetrahedron Lett.* **1981**, *22*, 1859−1862. (c) Alvaredo-Urbina, G.; Sathe, G. M.; Liu, W.-C.; Gillen, M. F.; Duck, P. D.; Bender, R.; Ogilvie, K. K. *Science* **1981**, *214*, 270−274.

(6) For recent reviews see: (a) Radhakrishnan, I.; Patel, F. J. *Structure* **1994**, *2*, 395−405. (b) Maher, L. J., III. *BioEssays* **1992**, *14*, 807−815. (c) Cheng, Y.-K.; Pettitt, B. M. *Prog. Biophys. Mol.Biol.* **1992**, *58*, 225−257. (d) Hélène, C. *Eur. J. Cancer* **1991**, *27*, 1466−1471.

(7) (a) Xodo, L. E.; Manzini, G.; Quadrifoglio, F. *Nucleic Acids Res.* **1990**, *18*, 3557−3564. (b) Kool, E. T. *J. Am. Chem. Soc.* **1991**, *113*, 6265−6266. (c) Prakash, G.; Kool, E. T. *J. Chem. Soc., Chem. Commun.* **1991**, 1161−1162. (d) Giovannangeli, C.; Monteney-Garestier, T.; Rougée, M.; Chassignol, M.; Thuong, N. T.; Hélène, C. *J. Am. Chem. Soc.* **1991**, *113*, 7775−7777. (e) Salunkhe, M.; Wu, T.; Letsinger, R. L. *J. Am. Chem. Soc.* **1992**, *114*, 8768−8772. (f) D'Souza,D. J.; Kool, E. T. *J. Biomol. Struct. Dyn.* **1992**, *10*, 141−152. (g) Trapane, T. L.; Ts'o, P. O. P. *J. Am. Chem. Soc.* **1994**, *116*, 10437−10438. (h) Noll, D. M.; O'Rear, J. L.; Cushman, C. D.; Miller. P. S. *Nucleosides Nucleotides* **1994**, *13*, 997−1005.

0002-7863/95/1517-12470$09.00/0

general strategy offers the opportunity to design new diagnostic probes, biochemical tools, and potential therapeutic agents that target (viral) messenger RNA ("antisense" strategy).

Several DNA triple helices have been characterized, which fall into two distinct classes depending on the mode of binding of the third strand to duplex DNA.[6,9] One of the most studied triplexes are those consisting of T*AT and C$^+$*GC triplets[2a,10] in which the third (T or C$^+$) strand is oriented *parallel* to the purine strand of the Watson–Crick duplex. In this case, the third strand lies within the DNA major groove and is held in place by *Hoogsteen* hydrogen bonds[11] to the purine strand. In the alternative motif, the third (purine-rich) strand binds *antiparallel* to the purine strand of the duplex through a *reverse-Hoogsteen* base-pairing scheme.[12] The best characterized triplets within this "antiparallel" motif are T·AT, G·GC, and A·AT. Thus, thymidine residues in the third strand (*T*) can be accommodated in both contexts, either in the "parallel" (*T**AT, Hoogsteen) or "antiparallel" (*T*·AT, reverse Hoogsteen) motifs (Figure 1).

Ab initio calculations predict that the energies of T*AT (parallel) and T·AT (antiparallel) base triplets differ by only 0.1 kcal/mol, in favor of the latter.[13] However, in oligonucleotides, additional stereochemical constraints and hydrophobic interactions favor the T*AT (parallel) bonding scheme.[4b,14] For example, dT_{10} binds to duplex dT_{10}/dA_{10} in the parallel (T*AT) scheme rather than the antiparallel (T·AT) orientation.[15] Furthermore, work originating from the laboratory of Fox and coworkers[16] and others[17] has elegantly demonstrated that T·AT triplets can form only when a few of such triplets are *interdispersed* between G·GC triplets. A stretch of *contiguous* T·AT triplets has been detected recently; however, its formation necessitated adjacent G·GC stretches, magnesium ions, and further stabilization by an acridine ligand.[16b] The location of the acridine intercalator was also critical, exerting its stabilizing effect only when positioned immediately adjacent to the G·GC stretch. In the absence of either the G·GC stretch, magnesium ions, or the acridine ligand, the complexes were not detected. This was explained by the suggestion that the acridine or the stretch of G·GC triplets alone does not provide a nucleation center strong enough to generate a stable T·AT stretch. The requirement of high G·GC content[17a] and divalent cations[18] for the stabilization of antiparallel (G·GC and T·AT) helices has also been recognized by others.

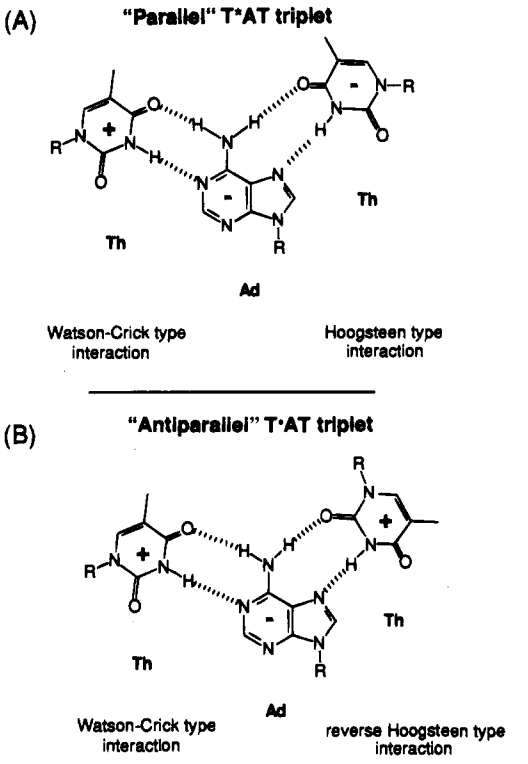

Figure 1. Configurations for the (A) T*AT and (B) T·AT triplex motifs. The + and − signs within the bases represent strand polarity and R the carbohydrate–phosphodiester backbone. The top T*AT triplet represents the more common motif wherein the third strand lies in the major groove *parallel* to the purine strand and conforms to the standard Hoogsteen H-bonding scheme (A). The representation on the bottom corresponds to the third strand occupying the major groove of the underlying double helix in an *anti-parallel* orientation, relative to the purine strand of the duplex (B).

Recent studies in our laboratory proposed the use of synthetic branched ("V" and "Y") oligonucleotides to (i) study the structure and role of naturally occurring branched RNA intermediates[19] and (ii) exploit their unique "forked" architecture to stabilize triple-helical structures.[20,21] In this paper, we show that a branched oligonucleotide with identical oligo(thymidine) chains linked to the 2′- and 3′-positions of a ribose branch-point nucleoside, i.e., $rA^{[2'-5'\text{-}dT_{10}]}{}_{3'-5'\text{-}dT_{10}}$ binds to dA_{10} to yield a triple-stranded complex containing only T·AT triplets. Fur-

(8) (a) Wang, S.; Kool, E. T. *J. Am. Chem. Soc.* **1994**, *116*, 8857–8858. (b) Reynolds, M. A.; Arnold, L. J.; Almazan, M. T.; Beck, T. A.; Hogrefe, R. I.; Metzler, M. D.; Stoughto, S. R.; Tseng, B. Y.;Trapane, T. L.; Ts'o, P. O. P. *Proc. Natl. Acad. Sci. U.S.A.* **1994**, *91*, 2433–2437. (c) Wang, S.; Kool, E. T. *Nucleic Acids Res.* **1994**, *22*, 2326–2333.

(9) Radhakrishnan, I.; Patel, D. J. *Biochemistry* **1994**, *33*, 11405–11416.

(10) (a) Miller, J. H.; Sobell, H. M.; *Proc. Natl. Acad. Sci. U.S.A.* **1966**, *55*, 1201–1205. (b) Morgan, A. R., Wells, R. D. *J. Mol. Biol.* **1968**, *37*, 63–80. (c) Lee, J. S.; Johnson, D. A.; Moran, A. R. *Nucleic Acids Res.* **1979**, *6*, 3073–3091. (d) Meervelt, L. V.; Vlieghe, D.; Dautant, A.; Gallois, B; Précigoux, G.; Kennard, O. *Nature* **1995**, *374*, 742–744.

(11) Hoogsteen, K. *Acta Crystallogr.* **1963**, *16*, 907–916.

(12) (a) Cooney, M.; Czernuszewicz, G.; Postel, E. H.; Flint, S. J.; Hogan, M. E. *Science* **1988**, *241*, 456–459. (b) Beal, P. A.; Dervan, P. B. *Science* **1991**, *251*, 1360–1363. (c) Durland, R. H.; Kessler, D. J.; Gunnell, S.; Duvic, M.; Pettit, B. M.; Hogan, M. E. *Biochemistry* **1991**, *30*, 9246–9255. (d) Chen, F.-M. *Biochemistry* **1991**, *30*, 4472–4479. (e) Pilch, D. S.; Levenson, C.; Shafer, R. H. *Biochemistry* **1991**, *30*, 6081–6087.

(13) Jiang, S.-P.; Jernigan, R. L.; Ting, K.-L.; Syi, J.-L.; Raghunathan, G. *J. Biomol. Struct. Dyn.* **1994**, *12*, 383–399.

(14) Escudé, C.; François, J.-C.; Sun, J.; Ott, G.; Sprinzl, M.; Garestier, T.; Hélène, C. *Nucleic Acids Res.* **1993**, *21*, 5547–5553.

(15) Pilch, D.; Levenson, C.; Shafer, R. *Proc. Natl. Acad. Sci. U.S.A.* **1990**, *87*, 1942–1946.

(16) (a) Fox, K. R. *Nucleic Acids Res.* **1994**, 22, 2016–2021. (b) Cassidy, S. A.; Strekowski, L.; Wilson, W. D.; Fox, K. R. *Biochemistry* **1994**, *33*, 15338–15347. (c) Washbrook, E.; Fox, K. R. *Nucleic Acids Res.* **1994**, *19*, 3977–3882. (d) Chandler, S. P.; Strekowski, L.; Wilson, W. D.; Fox, K. R. *Biochemistry* **1995**, *34*, 7234–7242.

(17) (a) Clarenc, J.-P., Lebleu, B.; Leonetti, J.-P. *Nucleosides Nucleotides* **1994**, *13*, 799–809. (b) Durland, R. H.; Rao, T. S.; Jayaraman, K.; Revankar, G. R. *Bioconjugate Chem.* **1995**, *6*, 278–282.

(18) (a) Milligan, J. F.; Krawczyk, S. H.; Wadwani, S.; Matteucci, M. D. *Nucleic Acids Res.* **1993**, *21*, 327–333. (b) Cheng, A.-J.; Van Dyke, M. W. *Nucleic Acids Res.* **1993**, *21*, 5630–5635. (c) Musso, M.; Van Dyke, M. W. *Nucleic Acids Res.* **1995**, *23*, 2320–2327.

(19) (a) Hudson, R. H. E.; Damha, M. J. *J. Am. Chem. Soc.* **1993**, *115*, 2119–2124. (b) Damha, M. J., Ganeshan, K., Hudson, R. H. E.; Zabarylo, S. V. *Nucleic Acids Res.* **1992**, *20*, 6565–6573. (c) Damha, M. J.; Zabarylo, S. V. *Tetrahedron Lett.* **1989**, *46*, 6295–6298. (d) Damha, M. J.; Ogilvie, K. K. *Biochemistry* **1988**, *27*, 6403–6416. (e) Damha, M. J.; Ogilvie, K. K. *J. Org. Chem.* **1988**, *53*, 3710–3722. (f) Damha, M. J.; Pon, R. T.; Ogilvie, K. K. *Tetrahedron Lett.* **1985**, *26*, 4839–4842.

(20) A brief account of this work has been presented at the Second International Symposium on Nucleic Acid Chemistry held in Sapporo, Japan, on Nov 9–11, 1993. See: (a) Hudson, R. H. E.; Damha, M. J. *Nucleic Acids Res. Symp. Ser.* **1993**, *29*, 97–99. (b) Hudson, R. H. E.; Ganeshan, K.; Damha, M. J. In *Carbohydrate Modifications in Antisense Research*; Sanghvi, Y. S., Cook, P. D., Eds.; ACS Symposium Series; American Chemical Society: Washington, D.C., 1994; Vol. 580, pp 133–152.

(21) Aside from our original reports (ref 20), two very recent reports exist in the literature on the use of branched oligonucleotides in (parallel) triplex DNA. See: (a) Azhayeva, E; Azhayev, A.; Guzaev, A.; Hovinen J.; Lonnberg, H. *Nucleic Acids Res.* **1995**, *23*, 1170–1176. (b) Wengel, J. *Bioorg. Med. Chem. Lett.* **1995**, *8*, 791–794.

ther, we demonstrate that short adenylate strands can bind *cooperatively* to the branched structure and provide, for the first time, the circular dichroism spectral "signature" of the T·AT (antiparallel) triplex.

Experimental Section

Synthesis of Oligonucleotides. Branched sequences were synthesized on an Applied Biosystems 381A instrument on a 1-μmol scale using β-cyanoethyl phosphoramidite chemistry[5b,22] as previously described.[19a,b] Purification, desalting, and analysis of the branched oligonucleotides by polyacrylamide gel electrophoresis were accomplished by our detailed protocols.[19b,23] Typical yields of branched oligomers were 5−15 A_{260} units (15−25%). The oligodeoxyadenylates were obtained from the University of Calgary DNA Synthesis Laboratory (Calgary, Alberta). The sequence 3′-$dT_{10}dC_4$5′−5′dT_{10}-3′ was prepared by assembly of 3′-$dT_{10}dC_4$-5′ on controlled-pore glass followed by "backward" 5′- to 3′-synthesis of the second dT_{10} segment. This necessitated a 5′-phosphoramidite 3′-dimethoxytritylated T monomer. Following deprotection, the oligomer bearing a terminal 5′-dimethoxytrityl protecting group was concomitantly detritylated and purified by reversed-phase column chromatography on trityl-on oligonucleotide purification cartridges (TOPC) according to the supplier's specifications (Applied Biosystems, Inc.).

Thermal Denaturation Profiles. Absorbance versus temperature profiles of complexes were measured at 260 or 284 nm with a Varian Cary I UV−vis spectrophotometer equipped with a Peltier temperature controller and interfaced with a computer. Data were collected with the spectrophotometer set on dual beam optical mode to reduce optical drift. The data were collected at 260 and 284 nm at 0.5 °C intervals with an equilibration time of 60 s for each measurement point. Extinction coefficients of the branched molecules were assumed to be similar to their corresponding linear sequences and were calculated from those of mononucleotides and dinucleotides according to the nearest-neighbor approximation.[24] Samples for thermal denaturation analysis were prepared by mixing the pyrimidine containing strand with the target, lyophilizing the solution to dryness, and dissolving the oligomers in the appropriate buffer. The mixtures were then transferred to Hellma QS-1.000-104 cells. Solutions contained ca. 2 μM of each oligomer in a buffer of (a) 10 mM Tris, 50 mM $MgCl_2$, pH 7.3 adjusted with HCl or (b) 1 M NaCl, 10 mM Na_2HPO_4, pH 7.0 adjusted with HCl. Oligonucleotide solutions were heated to 80 °C for 15 min and then slowly cooled to room temperature prior to melting experiments. Normalized plots were constructed according to the method of Kibler-Herzog et al.:[25] $[(A_t - A_o)/(A_f - A_o)]$, where A_o is the initial absorbance, A_f is the final absorbance, and A_t is the absorbance at any temperature. Hyperchromicity values (% H) are reported as the percent increase in absorbance at the wavelength of interest with respect to the final absorbance as described by Puglisi and Tinoco.[24] With the exception of branched **1**:dA_4 (1:1 and 1:2 ratio), which gave a broad thermal denaturation profile, all complexes showed sharp melting transitions. The melting temperature (T_m) was determined from the first derivative of each thermal curve. Precision in T_m values, determined from variance in repeated experiments, is no greater than ±0.5 °C.

Circular Dichroism Spectroscopy. Circular dichroic spectra were collected on a JASCO J-710 spectropolarimeter. Hellma fused quartz (165-QS) cells were used, and the temperature was controlled by an external constant temperature Neslab RTE-111 circulating bath. All spectra were recorded between 200 and 350 nm. The scan speed was 100 nm/min, sampling wavelength was 0.2 nm, and 15 repetitive scans were obtained and averaged for each sample. Solutions contained ca. 10 μM of each oligomer in a buffer of 10 mM Tris, 50 mM $MgCl_2$, pH 7.28 adjusted with HCl. Before data acquisition, samples were allowed to equilibrate for 10 min at the appropriate temperatures. The data were smoothed on a IBM/PC computer using Windows software supplied by JASCO, Inc. CD calculations were also performed with this software.

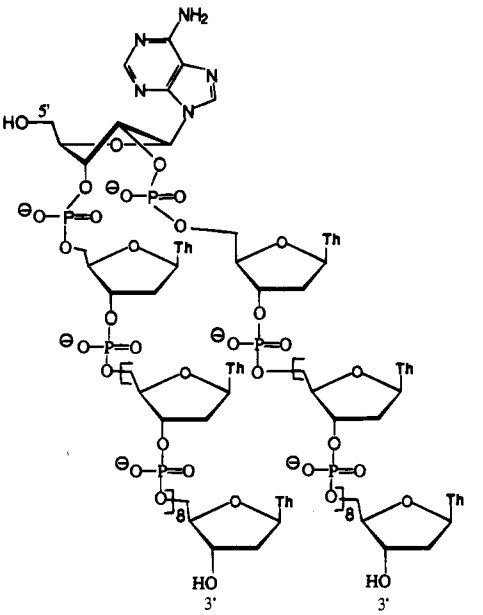

Figure 2. Primary structure of branched oligomer **1** showing the conformation of the branch-point adenosine unit as found in solution (ref 19d).

Stoichiometry Studies: Job Plots. The proportions in which (complementary) strands associate can be determined by titrating a solution of one strand with an equimolar (*ca.* 1 μM per strand) solution of the second strand as described by Job.[26] Titrations were performed in Hellma (Concord, ON) quartz micro cuvettes (QS-105, 10 mm path length). Absorbance measurements were collected on a Hewlett-Packard HP8452 spectrophotometer equipped with a thermostated cell holder controlled externally by a Lauda RMS-20 circulating bath. Solutions were allowed to equilibrate at 10 °C for 20 min prior to the first absorption measurement. Subsequent readings were made at 10 °C after each addition of complement strand.

Results and Discussion

Structure Considerations. The branched nucleic acid **1** was studied due to its relative simplicity, its ease of synthesis,[19a,b] and unique structural features (Figure 2). Recent studies on small branched RNA fragments, *e.g.*, the trinucleoside diphosphate $A^{[2'-5'dT]}{}_{3'-5'dT}$, indicate that the sugar−phosphate framework of the adenosine residue is rigid, a result of the strong base stacking between the adenine at the branchpoint and the adjacent 2′-thymine.[19d,27] The 2′−5′ and 3′−5′-phosphodiester linkages of $A^{[2'-5'dT]}{}_{3'-5'dT}$ are nearly parallel to one another and display significant preference for the ϵ^- and ϵ'^- conformation about the C2′−O2 and C3′−O3′ bonds (Figure 2).[19d] Also, the furanose ring of the adenosine residue shows a high preference for the C2′-endo pucker conformation ($^2E/^3E = 0.80$), a common feature of purine sugars linked to a pyrimidine via a 2′,5′-linkage.[28] These properties are also retained in larger branched molecules.[27] Thus, the branched nucleic acid **1** can be regarded topologically as a "V"-like or kinked structure, with the two dT_{10} strands oriented at a slight angle with respect to each other. The polarity of both dT_{10} strands is identical, 5′ → 3′ (from top

(22) Sinha, N. D.; Biernat, J.; McManus, J.; Koster, H. *Nucleic Acids Res.* **1984**, *12*, 4539−4557.

(23) Damha, M. J.; Ogilvie, K. K. In *Methods in Molecular Biology. Vol. 20: Protocols for Oligolnucleotides and Analogs*; Agrawal, S., Ed.; Humana Press, Inc.: Totowa, NJ, 1993; pp 81−114.

(24) Puglisi, J. D.; Tinoco, I., Jr. In Methods in Enzymology; Dahlberg, J. E., Abelson, J. N., Eds.; Academic Press, Inc.: San Diego, 1989; Vol. 180, pp 304−325.

(25) Kibler-Herzog, L.; Zon, G.; Whittierm, G.; Shaikh, M.; Wilson, W. D. *Anti-Cancer Drug Des.* **1993**, *8*, 65.

(26) Job, P. *Ann. Chim. (Paris)* **1928**, *9*, 113.

(27) Sund, C.; Agback, P.; Koole, L. H.; Sandstrom, A.; Chattopadhyaya, J. *Tetrahedron* **1992**, *48*, 695−718.

(28) (a) Kondo, N. S.; Holmes, H. M.; Stempel, L. M.; Ts'o, P. O. P. *Biochemistry* **1970**, *9*, 3479−3498. (b) Doornbos, J.; Den Hartog, J. A. J.; van Boom, J. H.; Altona, C. *Eur. J. Biochem.* **1981**, *116*, 403−412.

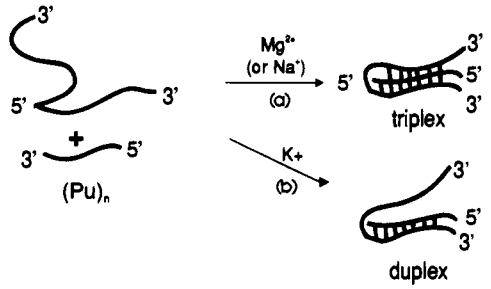

Figure 3. Comparison between triplex and duplex complexes involving compound **1** and dA_{10}. The "V" molecule is capable of forming a triplex in a Mg^{2+} or Na^+ buffer; however, with K^+ compound **1** forms a duplex containing a dangling (or "spectator") strand.

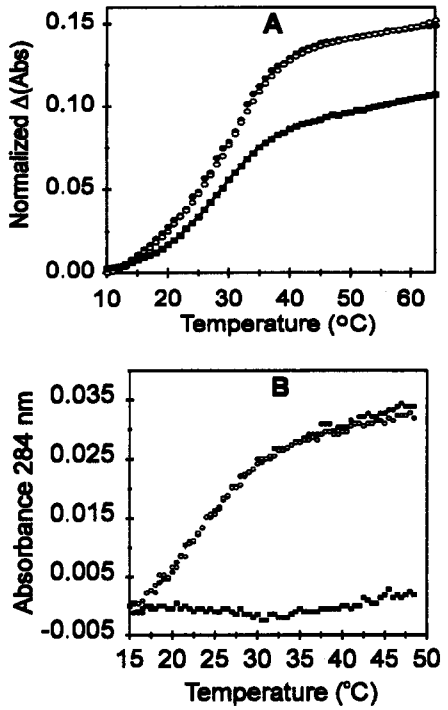

Figure 4. (A) UV absorbance melting curve (260 nm) for the complex formed between **1** (or dT_{10}) and dA_{10}: (−■−) T_{10}:dA_{10} 1:1; (−●−) **1**:dA_{10} 1:1; (−○−) **1**:dA_{10} 1:2. Normalized change in absorbance was calculated by $[(A_t - A_o)/(A_f - A_o)]$, where A_t = absorbance at any temperature, A_o= intitial absorbance, A_f = final absorbance. (B) Monitoring of melting at 284 nm. Symbols represent the same complexes as in A. Conditions for T_m determination are 1 M NaCl, 10 mM Na_2HPO_4, pH 7.0.

to bottom, Figure 2), and is a consequence of the solid-phase synthetic methodology.[19a,b] This characteristic makes **1** a highly attractive candidate for stabilizing the antiparallel T·AT triplex as it has the necessary parallel orientation for the dT strands found in this complex. Furthermore, the branched adenosine nucleotide provides a semirigid core that would favor a bimolecular triplex upon binding of **1** to dA_{10} (Figure 3A). This is an important structural feature since, as demonstrated below, the linear analogue 3′-$dT_{10}$$dC_4$-5′-5′-$dT_{10}$-3′ does not form a triplex with dA_{10}.

Interaction between 1 and dA_{10}. Stoichiometry. The melt curve at 260 nm for the complex formed between compound **1** and dA_{10} shows a monophasic, cooperative transition at 35.3 °C involving a hyperchromicity of 25% (50 mM $MgCl_2$, 10 mM Tris, pH 7.3). Similar results were obtained when the complex was studied in a Na^+ buffer system of high ionic strength (1 M NaCl, 10 mM Na_2PO_4, pH 7.0) (Figure 4, Table 1). Of note, the melting profile of **1**/dA_{10} shows a significantly greater hyperchromic rise than the melting of the dT_{10}:dA_{10} duplex under either Na^+ or Mg^{2+} conditions. This is attributed to the greater stacking interaction involved in a possible triple-stranded **1**/dA_{10} complex as compared to the double-stranded dT_{10}:dA_{10} complex. Addition of more dA_{10} to complex **1**/dA_{10} did not cause any change to the thermal denaturation profile, suggesting that **1** and dA_{10} interact in a 1:1 stoichiometry (Figure 4A). This is consistent with 1:1 stoichiometry as there was no further increase in hyperchromicity upon addition of further dA_{10}.

Table 1. Melting Transition Temperatures of Complexation by "V" (**1**) and Linear Oligonucleotides

components of complex	buffer system[a]	T_m[b] (°C)	% H[c]	curve shape
$A^{dT_{10}}{}_{dT_{10}}$ (**1**) + dA_{10}	S	32.8	20	monophasic
	M	35.3	25	monophasic
	P	19.0	8	monophasic
3′dT_{10}-dC_4-5′5′-dT_{10}3′ + dA_{10}	S	32.6	17	monophasic
	M	32.4	16	monophasic
T_{10} + dA_{10}	S	30.0	16	monophasic
	M	32.4	20	monophasic
$2T_{10}$ + dA_{10}	S	32.2	16	nonsigmodial[d]
	M	18.0, 33.2	18	biphasic
$A^{dT_{15}}{}_{dT_{15}}$ + dA_{10}	S	38.8	15	monophasic
	M	42.8	12	monophasic

[a] Conditions: S (sodium buffer) = 1 M NaCl, 10 mM PO_4^{3-}, pH 7.0; M (magnesium buffer) = 50 mM $MgCl_2$, 10 mM Tris, pH = 7.3; P (potassium buffer) = 140 mM KCl, 5 mM Na_2HPO_4, 1 mM $MgCl_2$, pH 7.2. [b] T_m's were determined from plots of the first derivative of absorbance against temperature. Error limits for individual measurements are estimated at ±0.5 °C in T_m. [c] % H values were calculated using the formula $[(A_f - A_o)/A_f]100$ where A_o = initial absorbance and A_f = final absorbance, with respect to the melt transition. [d] Slight asymmetry in low temperature region of the melt profile.

The stoichiometry of interaction of **1** with dA_{10} has been verified independently by titrating the branched oligomer with complement in the method of continuous variation.[26] The Job plots or mixing curves demonstrate that **1** and dA_{10} bind with 1:1 stoichiometry, regardless of the direction of titration for oligomer **1** and dA_{10} (Figure 5). This provides evidence that the complex involves both dT_{10} strands and is thus triple-helical. If only Watson−Crick interactions were involved, compound **1** would be expected to bind to 2 equiv of dA_{10}. However, because of the monophasic nature of the melt curve, it may be argued that the branched molecule is sterically inhibited and simply cannot simultaneously use both dT_{10} "arms" for hybridization. That is, the branched molecule is only capable of forming a duplex with one "arm" while the other "arm" remains a "spectator" (Figure 3B). However, several lines of evidence render this explanation improbable.

Monitoring Triplex Transitions at 284 nm. It is well documented that A−T Watson−Crick duplexes do not display changes in absorbance when their melting transition are monitored at 284 nm since, at this wavelength, they share a (virtual) isosbestic point with the melted duplex (i.e., single stranded dA_{10} and dT_{10}).[7ce,15,29−33] Triplex transitions, on the other hand, display changes in absorbance at both 260 and 284

(29) Riley, M.; Maling, B.; Chamberlin, M. J. *J. Mol. Biol.* **1966**, *20*, 359−389.
(30) Blake, R. D.; Massoulie, J.; Fresco, J. R. *J. Mol. Biol.* **1967**, *30*, 291−308.
(31) Pilch, D. S.; Brousseau, R.; Shafer, R. H. *Nucleic Acids Res.* **1990**, *18*, 5743−5750.
(32) Durland, M.; Peloille, N. T.; Thuong, N. T.; Maurizot, J. C. *Biochemistry* **1992**, *31*, 9197−9204.
(33) Fossella, J. A.; Kim, Y. J.; Shih, H.; Richards, E. G.; Fresco, J. R. *Nucleic Acids Res.* **1993**, *21*, 4511−4515.

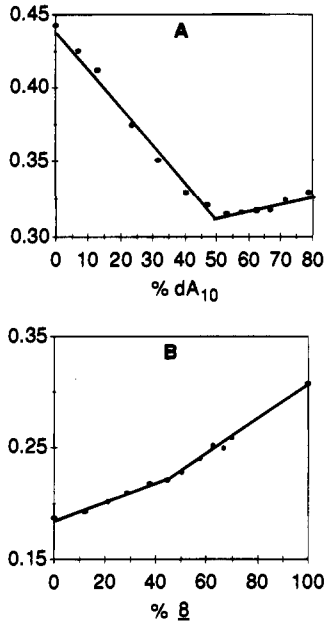

Figure 5. Determination of the stoichiometry of interaction for **1** and dA_{10} by the method of continuous variation (ref 26). In A the adenylate is added to a solution containing **1**, whereas in B **1** is added to a solution containing dA_{10}. The ordinate axis is in absorbance units at peak absorbance (*ca.* 260 nm). Conditions for stoichiometry determination are 50 mM $MgCl_2$, 10 mM Tris, pH 7.3.

nm, e.g., triplex → single strands,[7ce,32,34] or triplex → duplex + single strand.[15,31-33] Thus, by measuring melting profiles at 284 nm it is possible to observe a triplex transition independently from a A−T duplex transition. This is demonstrated by the melting curve of dA_{10}:dT_{10} duplex shown in Figure 4B. At 50 mM $MgCl_2$, or 1 M NaCl, a 1:1 mixture of dA_{10} and dT_{10} exhibited a monophasic helix-coil transition at 260 nm (Figure 4A) and no observable transition at 284 nm (Figure 4B).[15,32] Monitoring complex **1**/dA_{10} at 284 nm in either Na^+ (Figure 4B) or Mg^{2+} buffers shows clear melting transitions of small but significant hyperchromicity and confirms that, under these conditions, both the 2′- and 3′-dT_{10} "arms" in **1** are involved in the binding of a dA_{10} single strand. The linear oligomer 3′-$dT_{10}dC_4$-5′−5′-dT_{10}-3′, having also the appropriate polarity of dT strands but lacking the rigid branched framework, did not form a triplex, as judged by its circular dichroism spectrum (*vide infra*) and "flat" melt curve at 284 nm (data not shown). This result suggests that the rigidity of the branched core in **1** contributes significantly to the stabilization of the triplex. A related phenomenom is the remarkable stability of parallel Py*Pu:Py complexes formed between single-stranded purine oligonucleotides and triple-helix forming oligonucleotides containing a rigid terephthalamide unit.[7e]

Nature of the Triplex to Coil Transition. Commonly, triplex dissociation occurs through a two-step mechanism, i.e., dissociation of the triplex to a duplex and single strand, followed by dissociation of the duplex to single strands. Each process may show a separate transition in the thermal melt profile when resolved by sufficiently differing T_m's. For example, for the canonical dT_{10}*dA_{10}:dT_{10} (parallel) triplex, melting or displacement of the Hoogsteen third strand was observed as a separate event (T_m 17 °C) to the melting of the underlying duplex (T_m 30 °C) (5 mM Mg^{2+}, 10 mM PO_4^{3-}) (Table 1).[15,31] However, we have been unable to observe a clear biphasic profile for **1**/dA_{10} that would suggest an intermediate dissociation step (50 mM Mg^{2+} or 0.2−1 M Na^+). This behavior most likely arises in part from the intramolecular nature of the triplex; i.e., following the binding of one dT-"arm" to the target (Watson−Crick pairing), the effective local concentration of the other dT-"arm" is increased as to promote (reverse-Hoogsteen) binding to the adjoining duplex. The sharpness of the transition observed at 260 (and 284) nm indicates cooperativity between these two processes, e.g., via a "nucleation-zipping" mechanism.[35] Similar (one-step) cooperative transitions were observed for the "fold-back" oligomer 5′-dT_{10}-$dCTC_2$-dT_{10}-3′[36] and for circular[7b,c,f,8a] and other structurally altered nucleic acids.[7e,32,34,36] It is noteworthy that whatever the type of ion, Mg^{2+} or Na^+, the T_m value for complex **1**/dA_{10} is *ca.* 3 °C higher than that for the dT_{10}:dA_{10} duplex, which models the Watson−Crick duplex that can form in **1**/dA_{10} (Table 1). In addition to providing further evidence that both dT_{10} strands in **1** are involved in base-pairing interactions, this result shows that binding of one dT_{10} arm appears to enhance the thermal stability of the underlying duplex. A strikingly similar melting behavior has been observed for the intermolecular [$d(G_3A_4G_3)$·$d(C_3T_4C_3)$:$d(G_3A_4G_3)$] "anti-parallel" triplex.[12e]

It has been recently found that moderate concentrations of potassium cations, such as those present under physiological conditions (140 mM), inhibit the formation of "anti-parallel" triple-stranded DNA.[18] Therefore, we chose to investigate whether it was possible to observe under these conditions two separate transitions during the melting of **1**/dA_{10} or perhaps a single melt transition that was consistent with duplex melting. Mixtures of **1** and dA_{10} (1:1) and dT_{10} and dA_{10} (1:1) were incubated in a buffer containing 140 mM KCl, 5 mM Na_2HPO_4, and 1 mM $MgCl_2$ (pH 7.2), ionic concentrations known to inhibit triple-helix formation[18] and which are representative of intracellular conditions.[37] Complex formation was monitored by measuring melting profiles at 260 and 284 nm. Both complexes exhibited similar monophasic helix-coil transitions at 260 nm (ca. T_m 19.0 °C, %H = 8) and no observable transition at 284 nm, indicating that a duplex formed in both instances (**1**/A_{10}, Figure 6). These results, together with the CD studies described below, support the "spectator" T-strand model for the interaction of **1** and dA_{10} under these conditions (Figure 3B).

Circular Dichroism Studies. Triplex formation between **1** and dA_{10} was further supported by circular dichroism (CD) measurements. The CD spectra of **1**, dA_{10}, and the control oligomer dT_{10} are shown in Figure 7A.

Compound **1** (5 °C) shows a CD spectrum qualitatively similar to dT_{10} with a strong positive long wavelength Cotton effect at 287 nm and a weaker negative effect at 244 nm and a cross-over at 257 nm, which occurs near the maximum of the UV absorbance. The position of the major positive CD band at 288 nm is considerably red-shifted relative to that of dT_{10} (281 nm) and linear 11-mer dAT_{10} (279 nm, not shown). Complex formation is readily monitored by changes in both the amplitude and position of the CD bands. The CD spectrum of a 1:1 mixture of dA_{10} and dT_{10} at 5 °C (i.e., below duplex T_m) is characterized by maxima at 226, 263, and 284 nm as well as two minima at 247 and 268 nm (Figure 7C, g). The spectrum of dT_{10}*dT_{10}:dA_{10} at 5 °C is similar and characterized with a broader and smaller positive band at 227 nm (Figure

(34) Rumney, S.; Kool, E. T. *J. Am. Chem. Soc.* **1995**, *117*, 5635−5646.

(35) (a) Craig, M. E.; Crothers, D. M.; Doty, P. *J. Mol. Biol.* **1971**, *62*, 383−401. (b) Rougée, M; Faucon, B.; Mergny, J. L.; Barcelo, F.; Giovannangeli, C.; Garestier, T.; Hélène, C. *Biochemistry* **1992**, *31*, 9269−9278.

(36) Uddin, A. H.; Roman, M. A.; Anderson, J. R.; Damha, M. J. *J. Chem. Soc., Chem. Commun.*, in press.

(37) Alberts, B. In *Molecular Biology of the Cell*; Garland: New York, 1989; p 304.

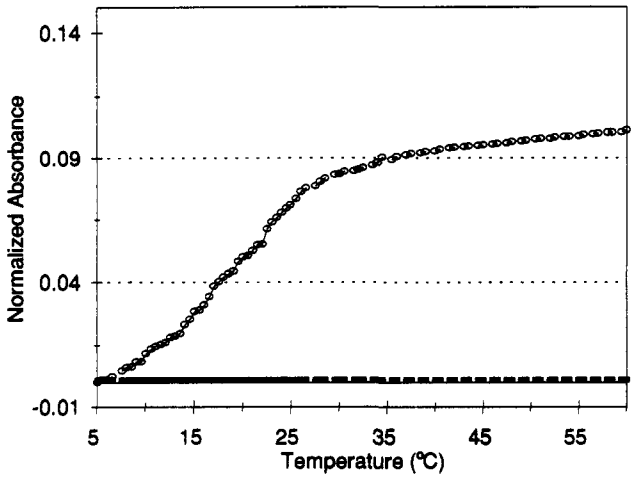

Figure 6. UV absorbance melting profile for the complex formed between **1** and dA_{10} monitored at 260 nm (−○−) and 284 nm (−■−) in physiological buffer (140 mM KCl, 5 mM Na_2HPO_4, 1 mM $MgCl_2$, pH 7.2). Normalized change in absorbance was calculated by $[(A_t - A_o)/(A_f - A_o)]$, where A_t = absorbance at any temperature, A_o = initial absorbance, A_f = final absorbance.

7C, f). This feature is believed to be indicative of triplex formation for this particular sequence.[31,32,38]

The 1:1 mixture **1**/dA_{10} in Mg^{2+} (60 °C) displays a spectrum that is similar to a superimposition of the spectra of the free, single-stranded **1** and dA_{10} (Figure 7B, d). When the temperature is decreased from 60 to 5 °C (**1**/dA_{10} in triplex form), the Cotton effects show a marked amplitude decrease with a slight red shift for the band at 287 nm (Figure 7B, e). The 5 °C spectrum of this complex is different from the CD spectra for the dT_{10}:dA_{10} duplex (Figure 7C, g) and parallel dT_{10}*dT_{10}:dA_{10} (Figure 7C, f) and [5′-dT_{10}-$dCTC_2$-dT_{10}-3′]:dA_{10} triplexes and cannot be assigned to any canonical form of DNA. Furthermore, it cannot be explained as the sum of the spectra of dT_{10}:dA_{10} duplex and dT_{10} at 5 °C. We consider this to be strong evidence in favor of the **1**/ dA_{10} complex being a triple helix and having a conformation with respect to base pair stacking and third strand orientation that is different to that of the canonical T*AT triplex.[4b]

As shown in Figure 7D, the CD spectra of 3′-$dT_{10}dC_4$5′−5′dT_{10}-3′/dA_{10} (Mg^{2+}) and **1**/dA_{10} (K^+) are similar to that of the dT_{10}:dA_{10} duplex (Mg^{2+}), indicating that a duplex-stranded helix was formed in both instances, as determined by their thermal denaturation profiles.

Effect of Target Chain Length and Sequence. Further evidence for compound **1** forming a triple-helical structure comes from measurements of complex stability with oligoadenylates of different chain lengths (dA_n). Figure 8 lists the melting temperatures of several **1**/dA_n complexes as well as those for the model dAT_{10} (**2**):dA_n duplexes. The melting curves of all complexes involving **1** showed a single inflection at 284 nm, indicating that bimolecular triplexes are formed. Examination of the data leads to the following conclusions: For complexes involving the branched oligomer **1** and dA_n, the T_m is linearly dependent on the target chain length (n) over a limited range. With regard to the melting of the duplexes, the changes in T_m are less sensitive to n. Note that, at $n = 10$, both lines change slopes, which corresponds to the number of thymines present in **2** and in each of compound **1**'s dT "arms". Beyond this value, the T_m's of the complexes remain linearly dependent on n ($10 \leq n \leq 20$), although the "V" line is still the most steep. This most likely reflects differences in the stability of the complexes and supports the idea that, in the case of **1**/dA_n, the adenylate strand is held to one dT_{10} strand by Watson−Crick bonding *and* to the other strand by reverse-Hoogsteen bonding. The increasingly higher T_m values beyond $n = 10$ are most likely the effect of stability as a result of reduced "fraying" at the ends of the complexes.[39] Another possible source of enhanced affinity as the dA_n segment increases is the expected effect of "sliding degeneracy".[40] This refers to the possibility of multiple positions of binding of "V" (**1**) on an dA_n template ($n > 10$) or of dA_n on a "V" (**1**) template ($n < 10$). These hypotheses receive additional support from the observation that the complex formed by dA_{10} and the analog with dT_{15}-"arms", i.e., $rA^{2'-5'\text{-}[dT_{15}]_{3'-5'dT_{15}}}$, had a T_m which was 7.5 °C greater than that for the complex formed between dA_{10} and **1** (Table 1, Mg^{2+}).

Below $n = 5$, the thermal stability of the duplexes exceeds that of the branched triplexes. For example, the melting curve of a 1:1 mixture of linear dAT_{10} (**2**) and dA_4 showed a sharp single transition at 21 °C; however, the first sharp transition detected with compound **1** was with dA_5. Thus, five base triplets are the minimum requirement for triple helix formation, in agreement with recent studies with parallel triplexes.[35]

Binding to dA_5 (1 equiv) results in branched and linear complexes with comparable thermal stability (T_m 19 and 21.5 °C, respectively; Figure 9). Addition of another molar equivalent of dA_5 gives a considerably stronger branched complex, with a T_m which is 6 °C higher than the one formed with only one equivalent (Figure 9B). We attribute this cooperative interaction to the propagation of a conformational change (e.g., base stacking) between adjacent sites of the terminal adenosine residues. The high cooperative nature of the melt profile (Figure 9B) suggests that binding of the first dA_5 oligomer provides a strong nucleation center for, and *enhances*, binding of the other. This behavior is in contrast to that observed for the duplex, in which no significant change in the T_m is observed upon further addition of dA_5 (Figure 9A). However, for both duplex and triplex, we find the hyperchromicity associated with the 2× dA_5 cases is significantly greater than for the 1× dA_5 cases, consistent with the involvement of more bases in these complexes. *Cooperative effects* such as the one observed for the **1**/(2× dA_5) complex are well documented in the literature[6b,41,42] but, to the best of our knowledge, have not been reported for triplexes conforming to the antiparallel (or "purine") motif.

Proper base-pairing is important in the antiparallel T·AT triplex as shown by the experiments with "V" (**1**) and the mismatch targets dAAAAXAAAAA (X = T or G) (Table 2). A single mismatch resulting from substitution of dA by dT (or dG) leads to a decrease in T_m of 11−13 °C. Of note, the TTT "mismatch" is less destabilizing that the TGT "mismatch". Also, the hyperchromicity associated with dissociation in the fully complementary case is 25%, while in the mismatch cases it is 16−18%, consistent with the involvement of fewer bases in the complex. Interestingly, the corresponding decreases in T_m for the mismatch duplexes are more significant (ca. 17 °C) compared to the mismatched triplexes (Table 2). This was not expected since a mismatch in the purine strand of a triplex

(38) Xodo, L.; Alunni-Fabbroni, M.; Manzini, G.; Quadrifoglio, F. *Nucleic Acids Res.* **1994**, *22*, 3322−3330.

(39) Leijon, M.; Graslund, A. *Nucleic Acids Res.* **1992**, *20*. 5339−5343.

(40) We thank a reviewer for making this point clearly.

(41) (a) Strobel, S. A.; Dervan, P. B. *J. Am. Chem. Soc.* **1989**, *111*, 6956. (b) Colocci, N.; Distefano; M. D.; Dervan, P. B. *J. Am. Chem. Soc.* **1993**, *115*, 4468−4473. (c) Colocci, N.; Dervan, P. B. *J. Am. Chem. Soc.* **1995**, *117*, 4781−4787.

(42) Naylor, R.; Gilham, P. T. *Biochemistry* **1966**, *5*, 2722−2728.

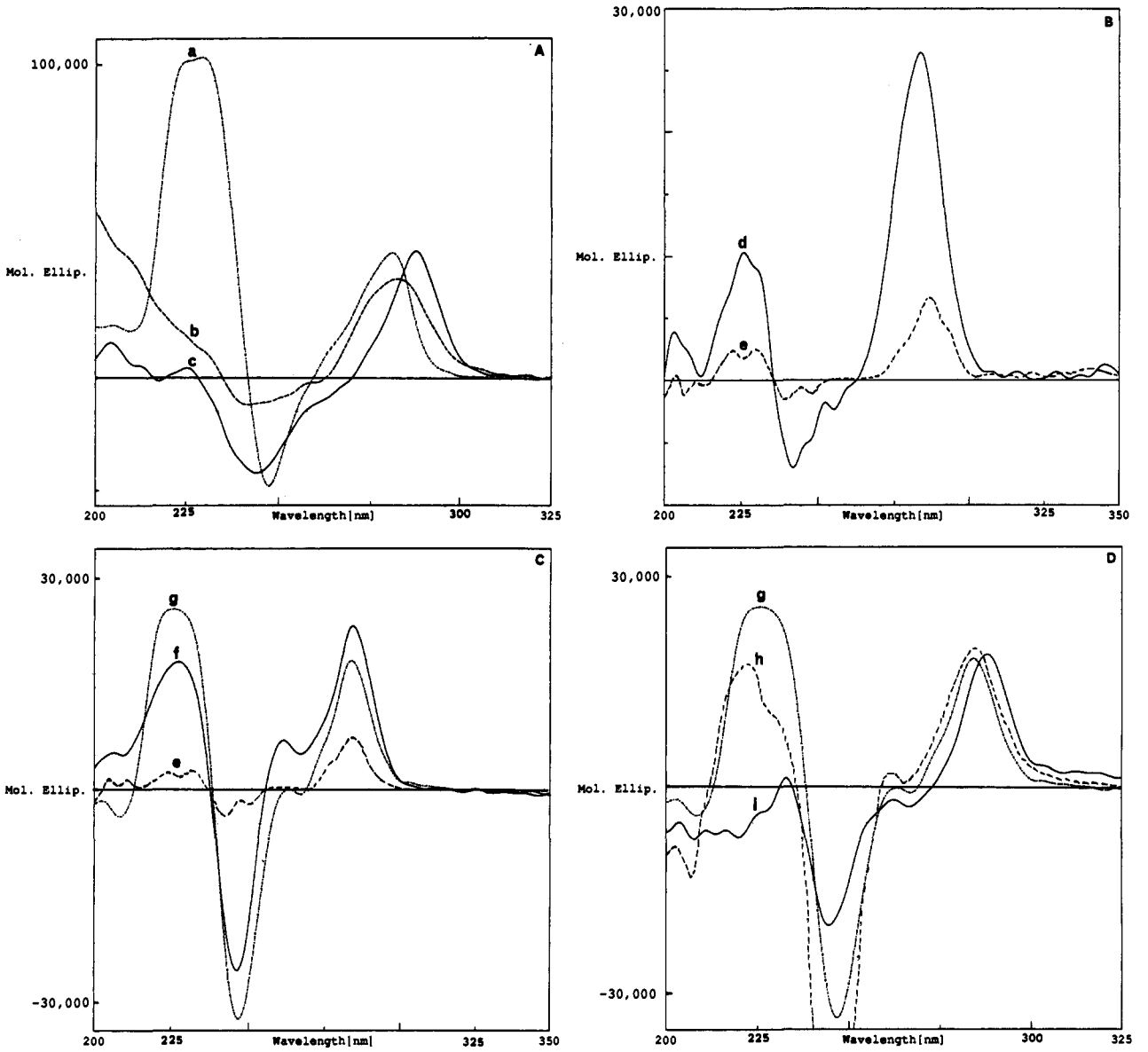

Figure 7. (A–D) CD spectra of (a) dA_{10} (5 °C), (b) dT_{10} (5 °C), (c) **1** (5 °C), (d) 1:1 **1**/dA_{10} (60 °C), (e) 1:1 **1**/dA_{10} (5 °C), (f) triplex dT_{10}*dA_{10}:dT_{10} (5 °C), (g) duplex dT_{10}:dA_{10} (5 °C), (h) 1:1 3′-$dT_{10}dC_4$5′-5′dT_{10}-3′:dA_{10} (5 °C), (i) 1:1 **1**/dA_{10} (5 °C) in K^+ buffer. Conditions for a–h: 50 mM $MgCl_2$, 10 mM Tris, pH. 7.3. Conditions for i: 140 mM KCl, 5 mM Na_2HPO_4, 1 mM $MgCl_2$, pH 7.2.

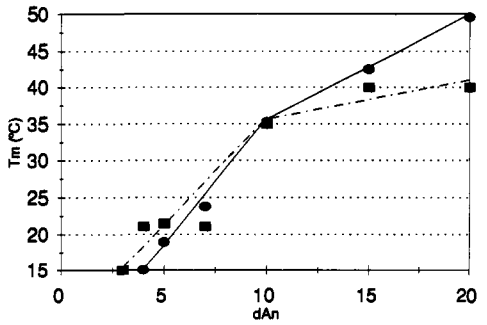

Figure 8. The effects of varying the adenylate chain length (n) on the melting temperature of complexes "V" (**1**)/dA_n (–●–), and dAT_{10} (**2**)/dA_n (–■–). Conditions: 50 mM $MgCl_2$, 10 mM Tris, pH 7.3.

structure would disrupt not only the Watson–Crick interaction but also the reverse-Hoogsteen interaction.[40] As a consequence, the destabilization for the triplex would be expected to be more pronounced as has been indeed reported for circular-DNA[7c] and other conformationally restricted,[7e] *parallel* triplex-forming systems. Thus, it is clear that for this particular *antiparallel* triplex structure (**1**:dA_{10}) the specificity of the base–base interactions is less stringent relative to an analogous *parallel* triplex.

Effect of the Branch Point. A question that arises in this study is whether all 10 T residues in **1** are involved in base-pairing interactions or whether the branch point prevents base pairing near it. These questions were addressed by comparing the melting temperatures of the complexes **1**:dA_{10} and **1**:dA_7 (complexes I and II, Figure 10). The significantly greater thermal stability of the former, combined with the slope-change observed at $n = 10$ in the T_m vs dA_n plot (Figure 8), indicates that near full-length base pairing can occur with dA_{10} complement. In addition, this result suggests that the branch point does not limit the "tail's" ability to hybridize with complementary nucleic acids.

Comparison of the thermal stability of complexes I (T_m 35.3 °C) and III (T_m 32.8 °C) confirms the proposition that the branch point does not present a significant deleterious steric or structural barrier. In addition, we find that the branched residue can base pair with a complementary residue in the target sequence, as suggested by the melting experiments with complexes III and

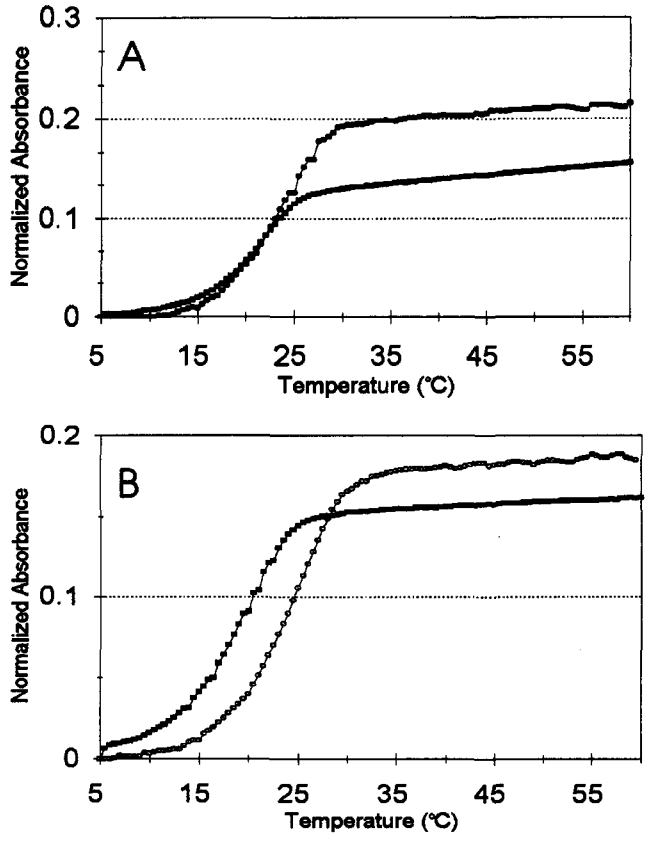

Figure 9. UV absorbance melting curves (260 nm) for dAT_{10} (**2**) (A), and "V" (**1**) (B) complexed with 1 equiv (−■−) and 2 equiv (−○−) of dA_5. Experimental conditions are the same as listed in Figure 8.

Table 2. Melting Temperatures (T_m) and Hyperchromicities (% H) for Fully Paired and Mismatched Complexes at pH 7.3[a]

oligomer	Target	T_m(°C)	% H
ATTTTTTTTTT	AAAAAAAAAA	34.7	17.4
	AAAATAAAAA	17.7	16.9
	AAAAGAAAAA	17.8	15.4
TTTTTTTTTT / A	AAAAAAAAAA	35.3	22.8
TTTTTTTTTT \ A	AAAATAAAAA	24.1	16.4
	AAAAGAAAAA	21.5	18.5

[a] Conditions: 50 mM $MgCl_2$, 10 mM Tris buffer. Error limits for individual measurements are estimated at ±0.5 °C in T_m.

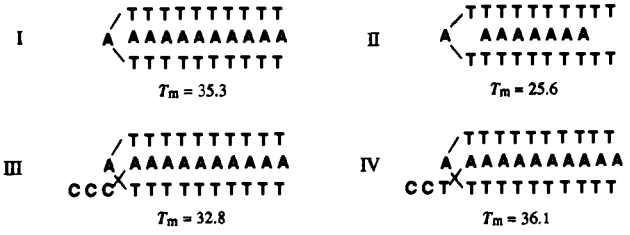

Figure 10. Effect on the target chain length and sequence on the T_m of branched complexes. Experimental conditions are the same as listed in Figure 8.

IV (Figure 10). The complex containing a rA/dC mistmatch (III) has a T_m which is 3−4 °C lower than that of the fully complementary complex (IV). This result indicates that interactions between the branch point residue and nucleotides of the target strand can in fact contribute to the stabilization of these triplexes. This observation is related to one described recently by Noll et al. in which a dT residue within a dT_4 loop connecting two homopyrimidine binding strands interacts with an dA residue in the target sequence.[43]

To further delineate the properties of the branched oligonucleotide probes, we synthesized the "Y" molecule 5′-dGCGTACTACGTT-rA[2′−5′-dT_{10}]$_{3′-5′-dT_{10}}$. The complex strengths were then compared for dA_{10} binding to the "V" (**1**) and "Y" (**3**) sequences. We find that the resulting complex with the "Y" oligomer has a T_m which is 3.5 degrees higher than with the "V" oligomer, establishing that its 5′-"arm" has a small but decisive stabilizing effect. The 5′-arm would be expected to reduce the overall degrees of freedom of the 2′ and 3′-dT_{10} strands and thus lead to enhanced stability (or reduced "breathing") of the triplex. We are currently investigating the influence of both the 5′-arm length and base sequence on the strength of binding with dA_{10} and other target sequences.

Relative Thermal Stability of (Parallel) T*AT versus (Antiparallel) T·AT Triplexes. In order to compare more quantitatively the relative stability of parallel and antiparallel TAT triplexes, we measured the melting temperatures of the "antiparallel" complex **1**:dA_{10} (T_m = 35 °C) and the bimolecular "parallel" complex [5′-dT_{10}-$dCTC_2$-dT_{10}-3′]:dA_{10} (T_m = 47 °C) in 50 mM $MgCl_2$, 10 mM Tris, pH 7.3 buffer. The significantly lower melting temperature of the **1**:dA_{10} complex (ΔT_m = 12 °C) is consistent with the general understanding of antiparallel py-pu-py triplexes that are not very stable and usually hard to observe.[16]

Conclusions

In this work, we have demonstrated that branched poly(pyrimidine) oligonucleotides can promote the formation of antiparallel T·AT triple helices. Due to the rigid structural features of branched oligonucleotides, triple-helices that are not stable enough to form in an intermolecular complex may be studied. This is particularly useful for complexes where structural data is not yet available. For example, our "branched" strategy may be used to induce the formation of the less common Pu*Pu:Py (Hoogsteen*Watson−Crick) triplexes, shown recently to form as intermediates during homologous recombination.[44] The parallel orientation of the (identical) purine strands in these complexes makes the branched oligonucleotides presented herein attractive probes to facilitate their study. Experiments designed to test this possibility are in progress.

Acknowledgment. We thank Dr. Richard T. Pon (University of Calgary) for providing oligodeoxynucleotide sequences and Dr. Joanne Turnbull (Concordia University) for assistance with the CD experiments. We acknowledge the Natural Science and Engineering Council of Canada (NSERC), the Canadian Foundation for AIDS Research, and Les Fonds pour la Formation de Chercheurs et l'Aide à la Recherche (FCAR) for support of this work. R.H.E.H. is the recepient of an NSERC postgraduate and postdoctoral scholarships and the 1995 Bio-Méga/Boehringer Ingelheim Award.

JA952675L

(43) Noll, D. M.; O'Rear, J. L.; Cushman, C. D.; Miller, P. S. *Nucleosides Nucleotides* **1994**, *13*, 997−1005.

(44) (a) Hsieh, P.; Camerini-Otero, C. S.; Camerini-Otero, R. D. *Genes Dev.* **1990**, *4*, 1951−1963. (b) Rao, B. J.; Dutriex, M.; Radding, C. M. *Proc. Natl. Acad. Sci. U.S.A.* **1991**, *88*, 2984−2988.